coatings

MDPI

Article

Selection of Optimum Binder for Silicon Powder Anode in Lithium-Ion Batteries Based on the Impact of Its Molecular Structure on Charge–Discharge Behavior

Norihiro Shimoi *, Masae Komatsu and Yasumitsu Tanaka

Graduate School of Environmental Studies, Tohoku University, 6-6-20 Aoba, Aramaki, Aoba-ku, Sendai 980-8579, Japan; masae.komatsu.c3@tohoku.ac.jp (M.K.); yasumitsu.tanaka.a8@tohoku.ac.jp (Y.T.)

* Correspondence: norihiro.shimoi.c8@tohoku.ac.jp; Tel./Fax: +81-22-795-4584

Received: 22 September 2019; Accepted: 4 November 2019; Published: 5 November 2019

Abstract: The high-capacity and optimal cycle characteristics of the silicon powder anode render it essential in lithium-ion batteries. The authors attempted to obtain a composite material by coating individual silicon particles of μm-order diameter with conductive carbon additive and resin to serve as a binder of an anode in a lithium-ion battery and thus improve its charge–discharge characteristics. Structural strain and hardness due to stress on the binder resin were alleviated by the adhesion between silicon or copper foil as a collector and the binder resin, preventing the systematic deterioration of the anode composite matrix immersed in electrolyte compositions including Li salt and fluoride. Moreover, the binder resin itself was confirmed to play a role of active material with occlusion and release of Li-ion. Furthermore, charge–discharge characteristics of the silicon powder anode active material strongly depend on the type of binder resin used; therefore, the binder resin used as composite material in rechargeable batteries should be carefully selected. Some resins for binding silicon particles were investigated for their mechanical and electrochemical properties, and a carbonized polyimide obtained a good charge–discharge cyclic property in a lithium-ion battery.

Keywords: Si powder anode; binder resin; adhesion; electrochemical property; lithium-ion battery

1. Introduction

Secondary cells such as lithium-ion and fuel cells are widely used as rechargeable batteries for home appliances [1–6], automobiles [7–14], smart houses [15–18], etc. These batteries can be made compact and highly efficient by designing them using high-capacity electrical energy and uniformly thin electrode (cathode and anode) films with a large area. Research focusing on the synthesis and selection of the active materials and conductive additives used in these batteries is being promoted. However, when using actual batteries (e.g., in an experiment), establishing a stable assembly technology for electrode composite materials using a wet process is necessary. In terms of compatibility between the active materials, conductive additives, and binders, the selection varies based on the combination, composition ratio, and application (batteries consisting of a solid [19–26], polymer [27–32], liquid electrolyte [25,31–37], etc.). However, there is no specific analysis of the impact of the binders' molecular structure and the combination of anode active materials on the charge–discharge behavior of rechargeable batteries. Thus, we used a binder resin, a matrix material supporting electrode active materials, and attempted to select an optimum structure for silicon (Si) powder anodes [38–43] to improve the electrochemical properties of lithium-ion rechargeable batteries.

It is assumed that the ideal structure for this binder, as a matrix that supports active materials and conductive additives, is a polymer that constitutes the binder spreading as a net and supporting

active materials and conductive additives. The Si anode undergoes repeated and rapid expansion and contraction due to the storage and release of lithium ions [44–47], thus separating from the binder. As a result, the binder is no longer able to support active materials and the electrode's structure collapses. This leads to the rapid deterioration of the charge–discharge behavior. Therefore, we chose various polymers based on commercially available Si powder (several micrometers in diameter), which are typically employed as binders in lithium-ion rechargeable batteries (Kojundo Chemical Laboratory Co., Ltd., Saitama, Japan), as anode active materials. We examined the impact of their molecular structures on the charge–discharge behavior of Si anodes.

With regard to anode active materials that use Si powder substrates, we propose herein an ideal electrode matrix structure that can improve the charge–discharge behavior of Si. Using multifaceted evaluation methods, we searched for a structure of binder resin that showed positive impacts on the charge–discharge behavior of Si powder anode active material.

Si, an active material of a rechargeable battery anode, shows charge–discharge behavior with a high capacity of approximately 4000 mAh/g [38], and is garnering attention as an active material for lithium-ion rechargeable battery anodes instead of graphite. Si, as an active material, repeatedly stores and releases lithium ions, but when lithium ions are incorporated into Si, the volume of the active material drastically expands [48] causing the rapid deterioration of the charge–discharge behavior. Presently, studies on suppressing such deterioration are being conducted [49], and charge–discharge behavior is being improved. However, the matrix structure that supports Si active material within electrodes is destroyed by volume expansion and contraction of Si, and thus it is difficult to support the electrode structure over a long period for practical use. Therefore, with a Si powder anode as the active material, a matrix structure is needed where electrode films can alleviate the stress even if there is expansion and contraction of Si. Figure 1 shows an ideal matrix structure that supports conductivity and ion conductivity, while being a buffer material for a volume change in Si active material, as a polymer matrix net. To build this structure, the selected binder should have a low electrochemical loss due to lithium consumption and a suppressed expansion of composite material due to expansion and contraction of active material. We therefore performed a thorough examination to select an optimum binder in terms of adhesion, extension, compression, and electrochemical properties.

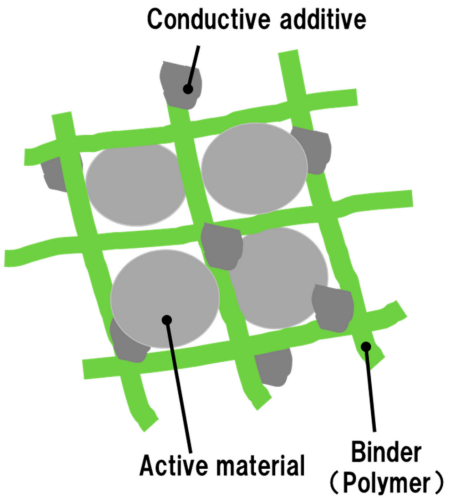

Figure 1. Ideal image of the anode composites with active materials, polymer, and conductive materials.

For our study, we chose some resins (binders) of polyvinylidene difluoride (PVDF), polyamide-imide (PAI), polyimide (PI), thermoplastic polyimide (TPI), polybenzimidazole (PBI), polyacrylonitrile (PAN), and polyacrylic acid (PAA) that are used as wet films for battery electrodes. Using the materials mentioned above as binders, we attempted to evaluate the mechanical and electrochemical properties of resins.

2. Experiments

2.1. Shear Peeling

We mixed and stirred Si powder (3N powder approximately 5 μm; Kojundo Chemical Laboratory Co., Ltd., Saitama, Japan) and a conductive additive (Ketjenblack®(KB) EJ300J; Lion Specialty Chemicals Co., Ltd. Tokyo, Japan) (weight ratio of Si:binder:KB, 1–25:1.5:1), and created a sample in Figure 2 by sandwiching it between Cu foils of 80 μm thickness (The Nilaco Corporation, Tokyo, Japan) for the shear peeling test. After sintering, the thickness of the binder film with Si powder and KB was 120 μm, and the sample was immersed in 40 °C electrolytes (1 mol/L lithiumhexafluorophosphate ($LiPF_6$), ethylene carbonate (EC): dimethyl carbonate (DMC): fluoroethylene carbonate (FEC): difluoroethylene carbonate (DFEC), 2:5:2:1 v/v%) for 3 h, and shear peeling strength was evaluated using a tensile test (load cell 5848; Instron Corporation, Norwood, Massachusetts, USA). As a result, we confirmed that, regardless of the electrolyte material compositions, adhesion improved with the added Si. In addition, we measured dependence of peel strength on electrolyte compositions (Li salt/fluoride) with 3.0 g of Si.

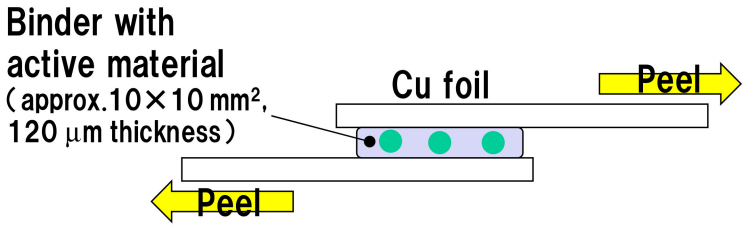

Figure 2. Cross-sectional image for shear peeling test. Ketjenblack®, KB.

Figure 3 shows the result of the shear peeling test. Polyvinylidene difluoride (PVDF) and polybenzimidazole (PBI) were peeled before being immersed in the electrolyte. There were notable differences for the other materials based on electrolyte immersion time, the amount of Si, and the presence/absence of Li salt in the electrolyte. Although the presence/absence of Li salt in the electrolyte did not have much impact on adhesion, the amount of Si in contact with the Cu foil and binder and the fluorine exposure time are considered important parameters.

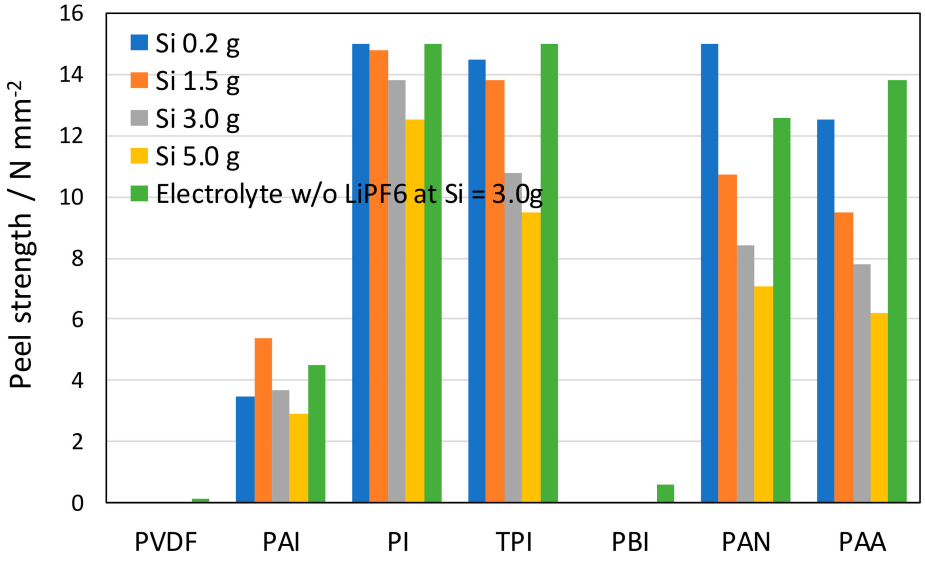

Figure 3. Comparison of peel strength for Si content within electrolyte. Polyvinylidene difluoride, PVDF; polyamide-imide, PAI; polyimide, PI; thermoplastic polyimide, TPI; polybenzimidazole, PBI; polyacrylonitrile, PAN; polyacrylic acid, PAA.

2.2. Compressive Strength

We prepared a pellet-type composite material with a 7 mm diameter and a 3 mm thickness with an electrode-like composition, and verified the composite strength of Si–resin adhesion strength and strength of resin alone through compression testing. Figure 4 shows the correlation between modulus of elasticity and strain rate of pellets due to compression before immersion and after 60 min of immersion in 40 °C electrolyte.

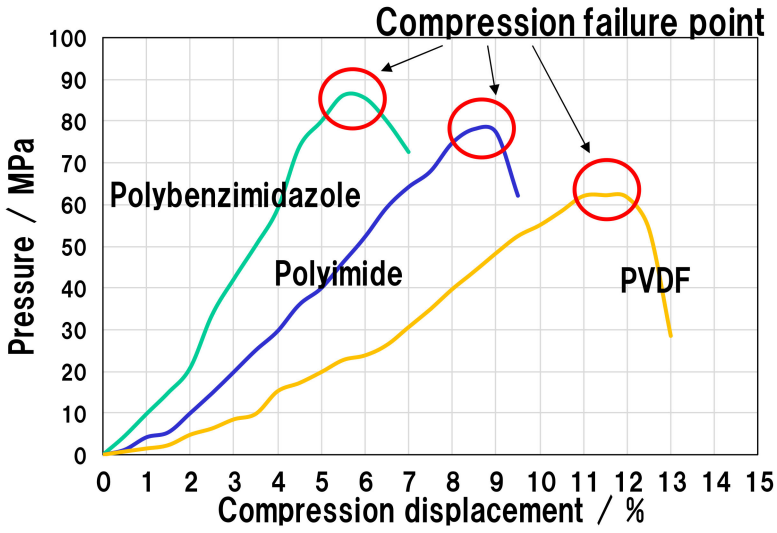

Figure 4. Comparison with compression displacement and deformation rate of a pellet.

Figure 5 shows the result of the above-described compression test. The pellet-type polyamide-imide (PAI), polyacrylonitrile (PAN), and polyacrylic acid (PAA) show attenuation of compression resistance due to electrolyte immersion. In addition, similar to the shear peeling test (Figure 2), compression resistance improved with the added amount of Si.

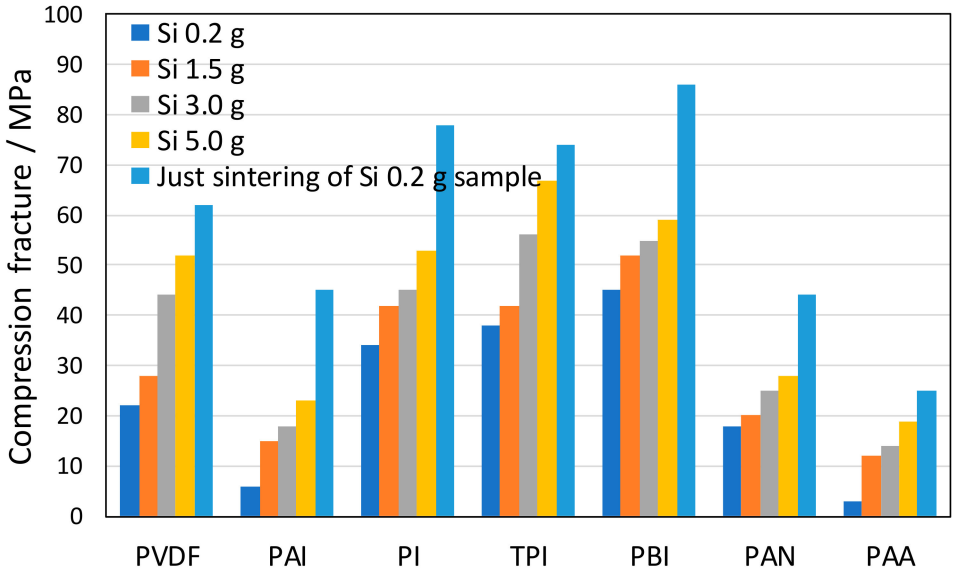

Figure 5. Dependence of compression fracture.

We further prepared a resin film (100 mm^2, 10 m thick), and soaked it in the electrolyte including EC, DMC, FEC, and DFEC at 40 °C for 2 h. Subsequently, we evaluated the rate of weight increase

after soaking (Figure 6). It showed that materials with simpler molecular structure had a higher expansion rate.

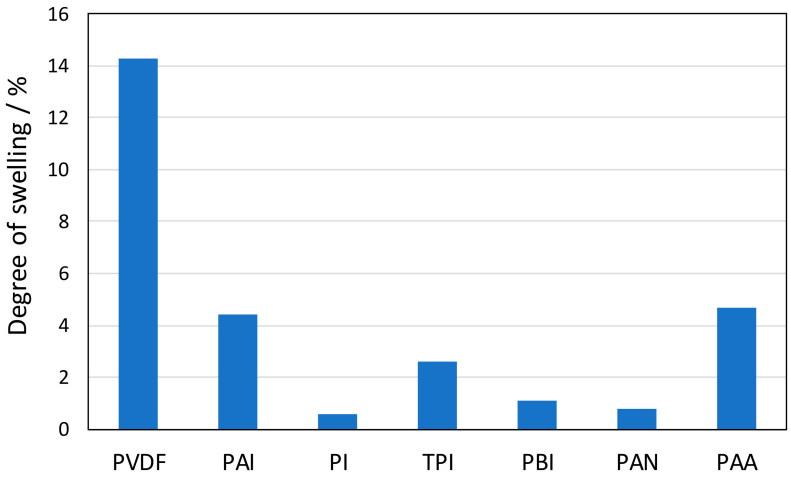

Figure 6. Comparison with degree of swelling.

2.3. Evaluation of Electrochemical Properties of Resins as Active Materials

We examined the dependence of charge–discharge properties on the binder resins. We evaluated the charge–discharge properties and cycle properties of retention, shown in Figure 7. For the anode, the mixing weight ratio of binder:conductive additive (copper powder; Kojundo Chemical Laboratory Co., Ltd., Saitama, Japan) was 1:8. Electrochemical testing of the composite anode electrodes was conducted using two-electrode 2032 type test coin cells (Housen Corporation, Osaka, Japan), caulking metal cups with a gasket to maintain the electrode assemblies, a polypropylene/polyethylene stacked film separator and a 1 M lithiumhexafluorophosphate ($LiPF_6$) electrolyte within solvents of DFEC/FEC/EC/DMC = 1/2/2/5 v/v%. The electrochemical performance of the two-electrode coin cells with $LiCoO_2$ cathode was evaluated using a potentiostat machine (Hokuto Denko Co. Ltd., Tokyo, Japan). The initial electrochemical performance of the composite anode in Figure 7a was evaluated in a coin cell using a constant current charge–discharge test in the voltage range of 0.3–2.0 V with a current density of 0.075 mA/cm^2 at room temperature. The state of the charge was set to 100%. The charge–discharge property of Figure 7a indicates the measured result using PI in an anode. We observed a tendency of the properties to change due to the binder resin in Figure 7b.

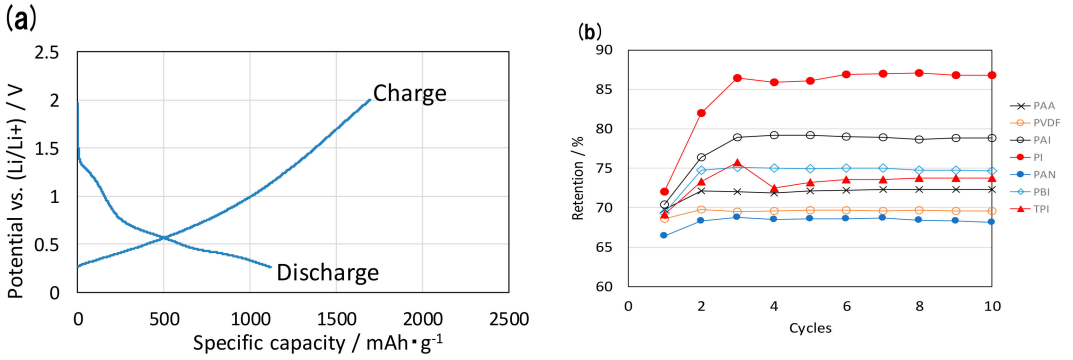

Figure 7. Electrochemical property of binder with Cu powder as conductive additive for cyclic characteristics. (**a**) Charge–discharge characteristics of polyimide (PI). Specific capacity indicates a capacity per weight of only PI included in an anode electrode of a 2032 type coin cell. (**b**) Retention of charge–discharge properties using binders as active materials in a 2032 type coin cell.

Each binder has a function of active material for the lithium-ion battery, and the irreversible capacity was large. In particular, binders, which had no benzene ring in the binder's molecular skeleton, had low retention, as shown in Figure 7b. It is presumed that a binder's benzene ring molecular structure had a role of occlusion and release of lithium ion in the graphite-like structure as anode active material.

Figure 8 shows the evaluation of the dependence of cycle properties on the composition of binder resins and the amount of conductive additives. A 2032 type coin cell using $LiCoO_2$ as a cathode electrode and a 1 M lithiumhexafluorophosphate ($LiPF_6$) electrolyte was used to evaluate the cyclic properties of charge–discharge. For the anode, the mixing ratio of Si power:binder:conductive additive (KB) was 10:1.5:1. The electrochemical performance of the composite anode shown in Figure 8 was evaluated in a coin cell using a constant current charge–discharge test in the voltage range of 1.6–4.1 V with a current density of 1.5 mA/cm^2 at room temperature. The state of the charge was set to 60%. We observed a tendency of the properties to change due to the binder resin in an anode electrode.

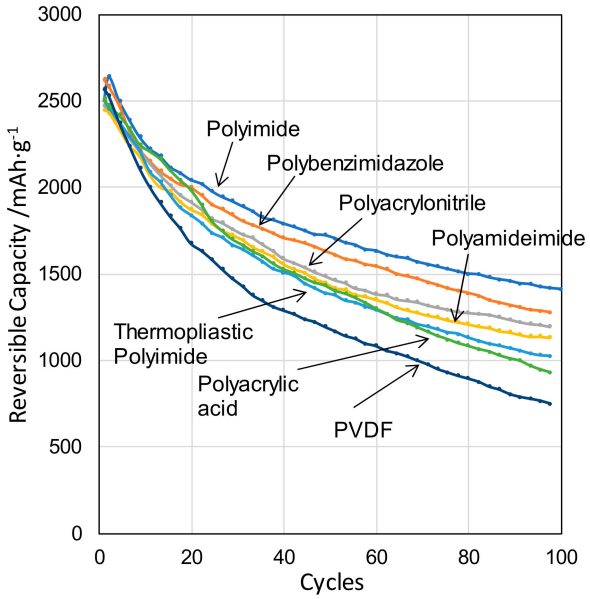

Figure 8. Dependence of binder with Si powder and conductive additive for cyclic properties.

The cross-sectional scanning electron microscopy (SEM) views with overviews of the anode electrode as insets in each SEM image of Figure 9 show the status of the anode electrodes after the 100th cyclic charge–discharge measurement. Figure 9a showing PVDF as a binder had an unclear boundary between Si powders and PVDF by the crystal collapse owing to the expansion and contraction of Si in the composite. It seems that the shape of Si powders in polyimide (PI) shown in Figure 9b was maintained; however, some small cracks on the surface of each Si powder occurred. It is believed that the binder layer covering each Si particle plays a buffering role by preventing cracking following drastic changes in volume with numerous repetitions of the charge–discharge cycle. We found that the polymer having large molecular structures and strong adhesion was effective in preventing the crystal collapse of Si by occlusion and exudation of Li-ion.

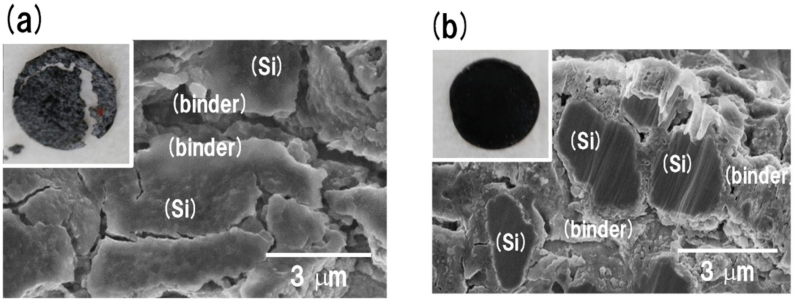

Figure 9. Overviews (inset in each scanning electron microscopy (SEM) views) and cross-sectional SEM views of anode electrodes with the composites of Si powder, Ketjenblack (KB) and binder ((**a**) PVDF, (**b**) PI) after 100th cycle. The dark area in each SEM image indicates Si active materials.

3. Results and Discussion

Figure 10 shows the correlation between the mechanical and electrochemical properties of the binder sample and the reversible capacity of the composite with binders, Si powder, and a conductive additive at the 100th cycle, as discussed and shown in Figure 8. Each sample was constructed (a) by sandwiching the composite of binders, Si powder, and a conductive additive between Cu foils for shear peeling strength, (b) using the pellet-type composite material including binders, Si powder and a conductive additive for compressive strength, and (c) using the composite with binders and copper powder for the retention at 10th cycle.

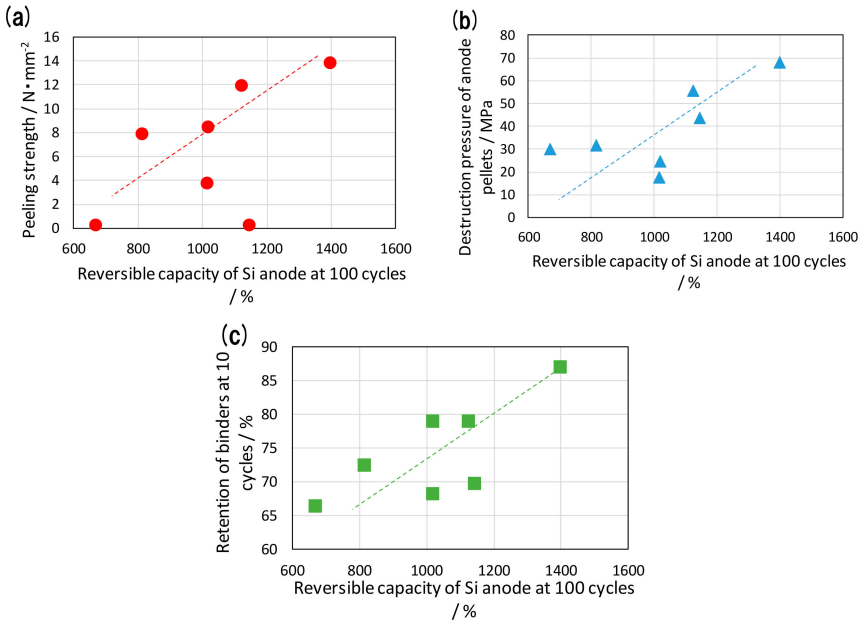

Figure 10. Correlation between mechanical and electrochemical properties of binders and inferiority of cycle property. (**a**) Peeling strength vs. reversible capacity of Figure 8 at 100th cycle. (**b**) Destruction pressure of anode pellets vs. reversible capacity at 100th cycle. (**c**) Retention of binders at 10 cycles vs. reversible capacity at 100th cycle.

The horizontal axis denotes the reversible capacity of Si powder, binder, and KB at the 100th cycle, and the vertical axis denotes (a) shear peeling strength and (b) compressive strength of each resin, and (c) retention between charge and reversible discharge of binders. It shows that cycle characteristics strongly depend on each of the mechanical and electrochemical measured results. This indicates that when the volume of the Si active material rapidly expands or contracts, the structural strain caused by

the stress on the binder resin is attenuated due to the adhesiveness between Si and the binder resin and the strength of the resin, preventing the systematic destruction of the matrix.

In the case of Si, the irreversible capacity during initial charge–discharge is about 20% of the total capacity [50]. To reduce the irreversible capacity of an electrode of a rechargeable battery, selecting a binder resin with low irreversible capacity is an important factor when designing an electrode.

When the electrode expands due to expansion in the Si volume while charging, the overall matrix, including the binder resin and conductive additive, also expands. Although the volumetric energy density changes as the electrode expands, there is no obvious correlation with the composition of the binder resin (i.e., resin strength).

Based on the molecular structures of each binder resin and the above-described experiment, we discovered that the type of side chain in PVDF, PAN, and PAA has a strong impact on material strength. In the case of PVDF, immersion in electrolytes containing fluorine leads to incompatibility with Si and rapid changes in the volume of the matrix that makes up the electrode. PAI, thermoplastic polyimide (TPI), and PBI have large structures but the main chain is asymmetrical, as shown in Figure 11, where solvents can easily enter the gap. These resins contain a six-membered ring and have high molecular weight, justifying their high hardness. Moreover, the asymmetrical structure leads to expansion in the electrolyte, which results in swelling as the electrolyte infiltrates. Furthermore, when hydrogen is present in the side chain, only relatively weak bonds, such as hydrogen bonds, exist with the dangling bond on the surface of Si, representing Van der Waals forces. In such cases, roughness on the surface of Si provides an anchoring effect in bonding, making it prone to peeling due to expansion and contraction of the substrate (Si) and insertion of fluorine between layers. On the other hand, if there is oxygen in the side chain, a relatively strong bond is supported by covalent bonding in Si. Thus, even when immersed in the electrolyte, adhesion with Si can be maintained, as shown in Figure 12.

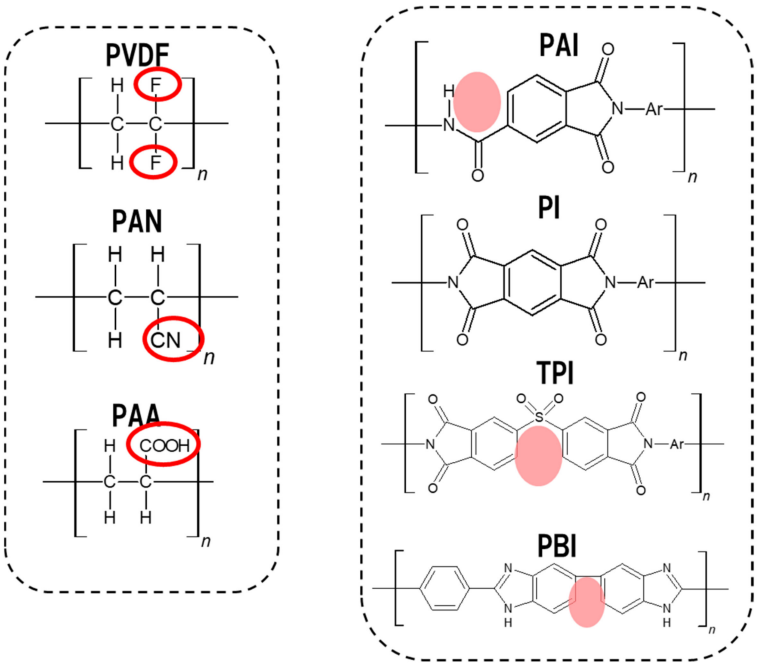

Figure 11. Schematic molecular skeleton image.

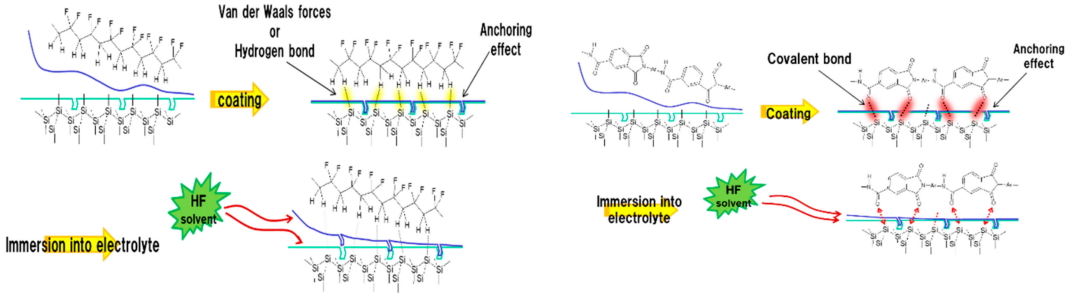

Figure 12. Adhesion image between Si surface and polymers.

Table 1 shows the comparison with electrical and ionic conductance between each binder. It is assumed that the electrical and ionic conductance between the active materials supported by the binder resin is regulated by the resin material. The specification of binders existing between the active materials impacts the electrical and ionic conductance between the active materials as an electrode, leading to an impact on cycle characteristics, as shown in Figure 8.

Table 1. Comparison with electrical and ionic conductance between each binder.

	PVDF, PAN, PAA	PI, PAI, TPI, PB
	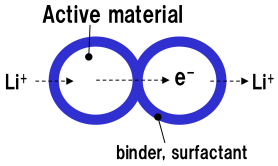	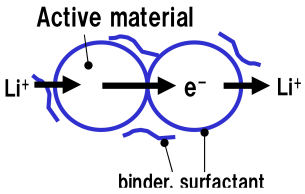
Electrical Conductance	Small	Large
Ionic Conductance	Small	Large

Based on the above evaluations, we successfully examined the dependence of charge–discharge behavior of active materials on binder resins. Through our study, we found that to obtain load characteristics that are relatively stable in a mechanical and electrochemical condition, the proper selection of molecular structure and composition for a matrix that supports Si active material is necessary. In short, the appropriate selection of molecular structure improves the charge–discharge behavior, presenting an idea for selecting binder resin for other active materials, in addition to Si.

4. Conclusions

In our study, we evaluated the mechanical and electrochemical behavior of binder resins used in anode active materials for rechargeable batteries. Specifically, adhesion of the binder resin and strength of the resin are responsible for improving the charge–discharge cycle characteristics of Si anode active material. This indicates that, during rapid volume expansion and contraction of Si active material, structural strain due to stress on the binder resin is alleviated by the adhesion between Si and the binder resin and hardness of the resin, preventing the systematic deterioration of the matrix. Furthermore, charge–discharge characteristics of Si anode active material strongly depend on the type of binder resin used; therefore, the binder resin used as composite material in rechargeable batteries should be carefully selected.

Author Contributions: Conceptualization, N.S.; methodology, M.K.; software, N.S.; validation, N.S., M.K. and Y.T.; formal analysis, N.S.; investigation, M.K.; resources, N.S. and Y.T.; data curation, N.S.; writing—original draft preparation, N.S.; writing—review and editing, N.S. and Y.T.; visualization, M.K.; supervision, N.S.; project administration, N.S.; funding acquisition, Y.T.

Funding: This research was funded by JSPS Grants-in-Aid for Scientific Research, grant number JP25630316 and the joint research fund was funded by DOWA Holdings Co., Ltd.

Acknowledgments: Our study was conducted with the support of FY2013-FY2014 grant-in-aid for Scientific Research "lithium-ion rechargeable battery active materials that apply single-layer nanosheet synthesis technology" (25630316) in association with DOWA Holdings in Japan.

Conflicts of Interest: The authors declare no conflict of interest.

References

1. Zubi, G.; Spertino, F.; Carvalho, M.; Adhikari, R.S.; Khatib, T. Development and assessment of a solar home system to cover cooking and lighting needs in developing regions as a better alternative for existing practices. *Sol. Energy* **2017**, *155*, 7–17. [CrossRef]
2. Akikur, R.K.; Saidur, R.; Ping, H.W.; Ullah, K.R. Comparative study of stand-alone and hybrid solar energy systems suitable for off-grid rural electrification: A review. *Renew. Sust. Energy Rev.* **2013**, *27*, 738–752. [CrossRef]
3. Bekele, G.; Palm, B. Feasibility study for a standalone solar-wind-based hybrid energy system for application in Ethiopia. *Appl. Energy* **2010**, *87*, 487–495. [CrossRef]
4. Carroquino, J.; Dufo-Lopez, R.; Bernal-Agustin, J.L. Sizing of off-grid renewable energy systems for drip irrigation in Mediterranean crops. *Renew. Energy* **2015**, *76*, 566–574.
5. Diouf, B.; Pode, R. Potential of lithium-ion batteries in renewable energy. *Renew. Energ.* **2015**, *76*, 375–380. [CrossRef]
6. Graham, V.A.; Hollands, K.G.T. A method to generate synthetic hourly solar-radiation globally. *Sol. Energy* **1990**, *44*, 333–341. [CrossRef]
7. Barre, A.; Deguilhem, B.; Grolleau, S.; Gerard, M.; Suard, F.; Riu, D. A review on lithium-ion battery ageing mechanisms and estimations for automotive applications. *J. Power Sources* **2013**, *241*, 680–689. [CrossRef]
8. Wagner, F.T.; Lakshmanan, B.; Mathias, M.F. Electrochemistry and the future of the automobile. *J. Phys. Chem. Lett.* **2010**, *1*, 2204–2219. [CrossRef]
9. Li, L.; Wu, Z.; Yuan, S.; Zhang, X.B. Advances and challenges for flexible energy storage and conversion devices and systems. *Energ. Env. Sci.* **2014**, *7*, 2101–2122. [CrossRef]
10. Goodenough, J.B. Evolution of strategies for modern rechargeable batteries. *Acc. Chem. Res.* **2013**, *46*, 1053–1061. [CrossRef]
11. Yuan, S.F.; Wu, H.J.; Yin, C.L. State of charge estimation using the extended kalman filter for battery management systems based on the arx battery model. *Energies* **2013**, *6*, 444–470. [CrossRef]
12. Zhang, C.; Li, K.; Pei, L.; Zhu, C.B. An integrated approach for real-time model-based state-of-charge estimation of lithium-ion batteries. *J. Power Sources* **2015**, *283*, 24–36. [CrossRef]
13. Mayyas, A.; Omar, M.; Hayajneh, M.; Mayyas, A.R. Vehicle's lightweight design vs. electrification from life cycle assessment perspective. *J. Clean. Prod.* **2017**, *167*, 687–701. [CrossRef]
14. Snoussi, J.; Ben Elghali, S.; Benbouzid, M.; Mimouni, M.F. Auto-adaptive filtering-based energy management strategy for fuel cell hybrid electric vehicles. *Energies* **2018**, *11*, 8. [CrossRef]
15. Dufo-Lopez, R.; Bernal-Agustin, J.L.; Yusta-Loyo, J.M.; Dominguez-Navarro, J.A.; Ramirez-Rosado, I.J.; Lujano, J.; Aso, I. Multi-objective optimization minimizing cost and life cycle emissions of stand-alone PV-wind-diesel systems with batteries storage. *Appl. Energy* **2011**, *88*, 4033–4041. [CrossRef]
16. Mulder, G.; De Ridder, F.; Six, D. Electricity storage for grid-connected household dwellings with PV panels. *Sol. Energy* **2011**, *84*, 1284–1293. [CrossRef]
17. Tong, S.; Fung, T.; Klein, M.P.; Weisbach, D.A.; Park, J.W. Demonstration of reusing electric vehicle battery for solar energy storage and demand side management. *J. Energy Storage* **2017**, *11*, 200–210. [CrossRef]
18. Delucchi, M.A.; Lipman, T.E. An analysis of the retail and lifecycle cost of battery-powered electric vehicles. *Transp. Res. Part D-Transp. Environ.* **2001**, *6*, 371–404. [CrossRef]
19. Goodenough, J.B. Challenges for rechargeable li batteries. *Chem. Mater.* **2010**, *22*, 587–603. [CrossRef]
20. Kasavajjula, U.; Wang, C.S.; Appleby, A.J. Nano- and bulk-silicon-based insertion anodes for lithium-ion secondary cells. *J. Power Sources* **2007**, *163*, 1003–1039. [CrossRef]

21. Wu, H.; Chan, G.; Choi, J.W.; Ryu, I.; Yao, Y.; McDowell, M.T.; Lee, S.W.; Jackson, A.; Yang, Y.; Hu, L.B.; et al. Stable cycling of double-walled silicon nanotube battery anodes through solid-electrolyte interphase control. *Nat. Nanotech.* **2012**, *7*, 309–314. [CrossRef] [PubMed]
22. Verma, P.; Maire, P.; Novak, P. A review of the features and analyses of the solid electrolyte interphase in Li-ion batteries. *Electochim. Acta* **2010**, *55*, 6332–6341. [CrossRef]
23. Komaba, S.; Murata, W.; Ishikawa, T.; Yabuuchi, N.; Ozeki, T.; Nakayama, T.; Ogata, A.; Gotoh, K.; Fujiwara, K. Electrochemical na insertion and solid electrolyte interphase for hard-carbon electrodes and application to na-ion batteries. *Adv. Func. Mater.* **2011**, *21*, 3859–3867. [CrossRef]
24. Bates, J.B.; Dudney, N.J.; Neudecker, B.; Ueda, A.; Evans, C.D. Thin-film lithium and lithium-ion batteries. *Solid State Ion.* **2011**, *135*, 33–45. [CrossRef]
25. Quartarone, E.; Mustarelli, P. Electrolytes for solid-state lithium rechargeable batteries: Recent advances and perspectives. *Chem. Soc. Rev.* **2011**, *40*, 2525–2540. [CrossRef]
26. Knauth, P. Inorganic solid Li ion conductors: An overview. *Solid State Ion.* **2009**, *180*, 911–916. [CrossRef]
27. Croce, F.; Appetecchi, G.B.; Persi, L.; Scrosati, B. Nanocomposite polymer electrolytes for lithium batteries. *Nature* **1998**, *394*, 456–458. [CrossRef]
28. Song, J.Y.; Wang, Y.Y.; Wan, C.C. Review of gel-type polymer electrolytes for lithium-ion batteries. *J. Power Sources* **1999**, *77*, 183–197. [CrossRef]
29. Meyer, W.H. Polymer electrolytes for lithium-ion batteries. *Adv. Mater.* **1998**, *10*, 439. [CrossRef]
30. Stephan, A.M. Review on gel polymer electrolytes for lithium batteries. *Euro. Poly. Jour.* **2006**, *42*, 21–42. [CrossRef]
31. Gadjourova, Z.; Andreev, Y.G.; Tunstall, D.P.; Bruce, P.G. Review of gel-type polymer electrolytes for lithium-ion batteries. *Nature* **2001**, *412*, 520–523. [CrossRef] [PubMed]
32. Horike, S.; Umeyama, D.; Kitagawa, S. ion conductivity and transport by porous coordination polymers and metal-organic frameworks. *Acc. Chem. Res.* **2013**, *46*, 2376–2384. [CrossRef] [PubMed]
33. Lewandowski, A.; Swiderska-Mocek, A. Ionic liquids as electrolytes for Li-ion batteries-An overview of electrochemical studies. *J. Power Sources* **2009**, *194*, 601–609. [CrossRef]
34. Le Bideau, J.; Viau, L.; Vioux, A. Ionogels, ionic liquid based hybrid materials. *Chem. Soc. Rev.* **2011**, *40*, 907–925. [CrossRef] [PubMed]
35. Osada, I.; de Vries, H.; Scrosati, B.; Passerini, S. Ionic-liquid-based polymer electrolytes for battery applications. *Angew. Chem. Int. Ed.* **2016**, *55*, 510–513. [CrossRef]
36. Yoshizawa, M.; Ogihara, W.; Ohno, H. Novel polymer electrolytes prepared by copolymerization of ionic liquid monomers. *Polym. Adv. Technol.* **2002**, *13*, 589–594. [CrossRef]
37. Armand, M. The history of polymer electrolytes. *Solid State Ion.* **1994**, *69*, 309–319. [CrossRef]
38. Netz, A.; Huggins, R.A.; Weppner, W. The formation and properties of amorphous silicon as negative electrode reactant in lithium systems. *J. Power Sources* **2003**, *119–121*, 95–100. [CrossRef]
39. Besenhard, J.O. *Handbook of Battery Materials*; Wiley-VCH: Weinheim, Germany, 1999.
40. Huggins, R.A. Materials science principles related to alloys of potential use in rechargeable lithium cells. *J. Power Sources* **2003**, *26*, 109–120. [CrossRef]
41. Obrovac, M.N.; Krause, L.J. Reversible cycling of crystalline silicon powder. *J. Electrochem. Soc.* **2007**, *154*, A103–A108. [CrossRef]
42. Liu, X.H.; Li, Z.; Shang, H.; Scott X., M.; Ting, Z.; Huang, J.Y. Size-dependent fracture of silicon nanoparticles during lithiation. *ACS Nano* **2012**, *6*, 1522–1531. [CrossRef] [PubMed]
43. Zhao, K.; Pharr, M.; Wan, Q.; Wang, W.L.; Kaxiras, E.; Vlassak, J.J.; Suo, Z.G. Concurrent reaction and plasticity during initial lithiation of crystalline silicon in lithium-ion batteries. *J. Electrochem. Soc.* **2012**, *159*, A238–A243. [CrossRef]
44. Park, C.M.; Kim, J.H.; Kim, H.; Sohn, H.J. Li-alloy based anode materials for Li secondary batteries. *Chem. Soc. Rev.* **2010**, *39*, 3115–3141. [CrossRef] [PubMed]
45. Hatchard, T.D.; Dahn, J.R. In situ XRD and electrochemical study of the reaction of lithium with amorphous silicon. *J. Electrochem. Soc.* **2004**, *15*, A838–A842. [CrossRef]
46. Li, H.; Huang, X.J.; Chen, L.Q.; Wu, Z.G.; Liang, Y. A high capacity nano-Si composite anode material for lithium rechargeable batteries. *Electrochem. Solid State Lett.* **1999**, *2*, 547–549. [CrossRef]
47. Birke, P.; Chu, W.F.; Weppner, W. Materials for lithium thin-film batteries for application in silicon technology. *Solid State Ion.* **1996**, *93*, 1–15. [CrossRef]

48. Kuiqing, P.; Jiansheng, J.; Wenjun, Z.; Shuit-Tong, L. Silicon nanowires for rechargeable lithium-ion battery anodes. *Appl. Phys. Lett.* **2008**, *93*, 033105.
49. Shimoi, N.; Qiwu, Z.; Bahena-Garrido, S.; Tanaka, Y. Mechanochemical approaches to employ silicon as a lithium-ion battery anode. *AIP Adv.* **2015**, *5*, 057142. [CrossRef]
50. Miyachi, M.; Yamamoto, H.; Kawai, H. Electrochemical properties and chemical structures of metal-doped sio anodes for li-ion rechargeable batteries. *J. Electrochem. Soc.* **2007**, *154*, A376–A380. [CrossRef]